Hydrodynamics of Kraft Lignins

T. M. Garver* and P. T. Callaghan

Department of Physics and Biophysics, Massey University, Palmerston North, New Zealand

Received July 19, 1989; Revised Manuscript Received June 15, 1990

ABSTRACT: The self-diffusion coefficients of kraft lignin preparations in aqueous and nonaqueous solvents have been measured by using pulsed field gradient NMR (PFGNMR). The diffusion coefficients of kraft lignin fractions conform to the relationship $D_s \sim M^{-\alpha}$, where α is 0.39 for unacetylated lignin in aqueous 1.0 M NaOD and 0.30 for acetylated lignins in $CDCl_3$. These exponents and the measured D_0 values indicate a branched macromolecule. Measurements of the concentration dependence of the self-diffusion coefficients for both the solvent and solute are consistent with an extremely compact and flat conformation for acetylated lignin in $CDCl_3$. A diffusion coefficient corresponding to a hydrodynamic radius of 380 Å in pH 6.5 aqueous buffer indicated significant association under these conditions. However, there was no evidence of association for unacetylated lignin preparations in pH 9.0 D_2O, aqueous 1.0 M NaOD, and DMF-d_7 and for acetylated lignins in $CDCl_3$ and acetone-d_6. A kinetic interpretation based on free-volume theory is given for diffusion of branched macromolecules in concentrated solution.

Introduction

Lignin is a structural macromolecule, found in conjunction with hemicellulose components between cellulose microfibrils, in the cell wall of vascular plants. Although lignin biosynthesis is currently perceived to occur by random coupling of free-radical intermediates derived from phenylpropanoid alcohols, the "polymerization" steps of lignin biosynthesis are poorly understood.[1] In fact, several recent reports have focused on the extent of order of the lignin macromolecule either in the plant cell wall environment or after removal from the cell wall by various pulping processes.[1-4] Kraft pulping is currently the most common method used for removal of the unwanted lignin component from wood during recovery of cellulose for the manufacture of paper products. As such, kraft lignins represent a significant potential resource. Kraft pulping cleaves and solubilizes the lignin under relatively severe aqueous conditions at 170 °C in 1 M NaOH and 0.2 M Na_2S.[3] Alder has reviewed the principal structures found in softwood lignins,[5] and Gierer has reviewed structural transformations known to occur during pulping processes.[6] Several significant phenylpropanoid structures found in kraft lignins, arising directly from native lignin structures, are depicted in Figure 1. In kraft lignins typically about 42% of the phenolic oxygens are not etherified and may be ionized in alkaline solution. This percentage decreases with increasing molecular weight.[7,8]

Motivation for PFGNMR Hydrodynamic Studies. Difficulties arising from lignin physical properties have notoriously impeded efforts to apply the techniques of light scattering, chromatography, viscosimetry, and tracer analysis to the systematic study of lignin hydrodynamics. The extent of these difficulties includes problems with fractionation and purification due to association and adsorption on chromatographic media as well as the spectrophotometric properties of lignin, which complicate light scattering due to ubiquitous absorbance and fluorescence bands.[9] The resulting deficiency of information has led to confusion about the branching and conformation of the lignin macromolecule and the conditions required for their association.[10,11] Association has resulted in difficulties in separation, and low internal mobility has limited subsequent NMR spectroscopic analysis, thereby frustrating efforts to investigate lignin macromolecular structure. The diffusion experiments reported here provide evidence distinguishing mobilities. In particular, the mobility arising from the hydrodynamic radius of the kraft lignin macromolecule is distinguished from that due to association. In subsequent paper the rotational diffusion and internal mobility will be discussed in terms of the implications and effect on NMR correlation times.[12]

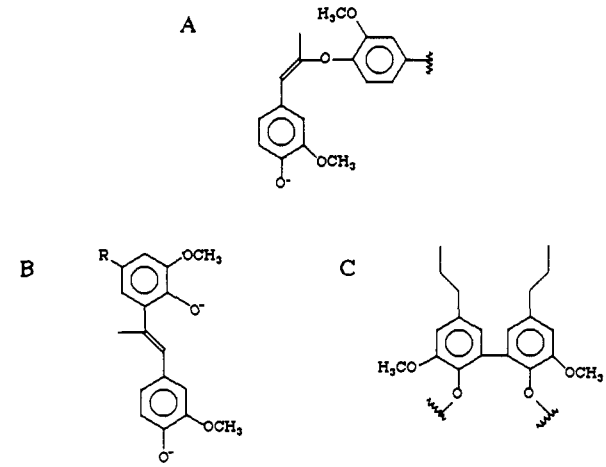

Figure 1. Representative structures indicating probable linkages between phenylpropane units in kraft lignin: (A) vinyl aryl ether derived from a β-O-4 structure; (B) *p,o'*-stilbene derived from phenylcoumaran structure; (C) 5,5 linkage between two guaiacyl units.[6]

While a principal motivation for this work is to improve our understanding of the mobility of kraft lignin solutions for the purposes of further structural analysis by a combination of chromatography and magnetic resonance techniques, we also clarify the extent of association and provide clear evidence concerning the incidence of branching in the lignin macromolecule.[10,11] Additionally, industrial processing of kraft lignins requires more fundamental information on the physical and structural properties of the lignins in kraft black liquor. Potentially, fundamental results on the hydrodynamics of kraft lignins may be applied to the study of the fluid dynamics of pulping processes[18] and kraft recovery operations. Association was

* Present address: Hamilton Hall, Department of Chemistry, University of Nebraska—Lincoln, Lincoln, NE 68588.

0024-9297/91/2224-0420$02.50/0

identified as contributing to very slow diffusion coefficients in aqueous solutions in an early study by Benko on lignosulfonates, which associated in 0.1 M KCl, and on kraft lignins, which associated upon dropping the pH from 11 to 7.[13] Other studies of the diffusion of lignosulfonates have led to the conclusion that the infinite-dilution diffusion coefficients scale to $M^{-0.33}$ as expected for a branched macromolecule or a "spherical microgel".[9] In 1960 Gupta and Goring published a series of articles on the hydrodynamic properties of alkali lignins as interpreted from data obtained with viscosimetric, light scattering, and sedimentation techniques.[14-16] At pH 9.65 Goring et al. found that these alkali lignins had molecular weights of 5×10^4 to 5×10^7 with z-average radii of gyration for the fractions typically 440 Å and up to 2600 Å.[16] Goring found that sedimentation coefficients and reduced viscosities of alkali lignins at pH 9.65 have values that correspond to compact structures. The Mark–Houwink exponent and the molecular weight dependence of the s values of alkali lignins at pH 9.65 were found to be between those expected for a sphere and a random coil.[16] Recently, Goring's laboratory has presented evidence that lignin exists in flat disk-shaped structures ca. 20 Å in thickness.[18,19] Our data conforms to Goring's 1971 review of the polymer properties of lignins indicating that kraft lignin is a branched macromolecule that readily associates in aqueous solutions under buffered neutral-pH conditions.[9,19] Our data also provide an analysis of the translational mobility of acetylated lignins in nonaqueous solvents. These are the kraft lignin derivatives and solvents most frequently studied by NMR spectroscopy. The nonaqueous solution experiments reported on here indicate an extremely compact macromolecule with a flat oblate ellipsoid conformation.

Pulsed Field Gradient NMR (PFGNMR). The attenuation of a spin echo due to diffusion in an inhomogeneous field was observed during Hahn's original spin-echo experiments[20] and was subsequently developed into a practical tool for the measurement of diffusion by Carr and Purcell[21] and Stejskal and Tanner.[22] The versatility and capability of pulsed gradient spin-echo NMR to directly measure polymer and solvent self-diffusion coefficients down to 10^{-14} m^2 s^{-1} have been reviewed elsewhere.[23-27] The PFGNMR diffusion experiment relies on the change in the spatial distribution of the proton spins between two precisely matched gradient pulses during a Hahn spin-echo experiment. The resulting echo attenuation is given by the Stejskal and Tanner equation

$$A(G)/A(0) = \exp[-D_s\gamma^2G^2\delta^2(\Delta - \delta/3)] \quad (1)$$

where D_s is the self-diffusion coefficient, γ is the magnetogyric ratio, and G is the imposed magnetic field gradient of duration δ with separation Δ between gradient pulses.[22] For a polydisperse sample with molar mass dependent self-diffusion coefficients, the observed echo is a molar mass weighted average. In general, the sum of echos will result in multiexponential decays. Assuming no molar mass dependence of T_2, this leads to a diffusion coefficient given by[28]

$$\bar{D}_s = \sum_i N_iM_iD_{si}/\sum_i N_iM_i \quad (2)$$

The diffusion measurements that we have made occur over a wide range of solvent conditions where the T_2 relaxation times vary by nearly 2 orders of magnitude from 8 to 300 ms. In order to minimize the effect of T_2 weighting, we have attempted to measure the diffusion coefficients using high gradients on spin echos formed at <16 ms.

Experimental Section

Preparation and Characterization of Lignin Samples. The preparation of *Pinus radiata* kraft lignin and the subsequent fractionation procedure using Superose (Pharmacia) and 0.10 M NaOH have been recently reported.[8] The molecular weights for the preparative fractions were obtained from direct calibration of a Superose-12 size exclusion column with 0.10 M NaOH as eluant. Sedimentation equilibrium was used to calibrate this column, using both preparative and analytical fractions.[8] The polydisperse lignin sample from which the fractions were derived had a molecular weight of 4520 and a polydispersity (M_w/M_n) of 3.2 as measured by these size exclusion experiments. The lignin fractions were acetylated by using freshly distilled pyridine, acetic anhydride, acetic acid, and water following the procedure given by Garver and Sarkanen.[7] In order to test for any significant aggregation due to dimerization of carboxylic acids, and acetylated lignin sample was methylated with diazomethane prepared in $CHCl_3$ (alcohol free) from Dialzald (Aldrich Chemical Co., Milwaukee, WI). The diazomethane preparation procedure was a modification of that reported by deBoer and Backer[29] using freshly distilled 2-(2-methoxyethoxy)methanol and chloroform as the reaction cosolvents with the aqueous KOH solution.[30] After methylation the sample was washed five times with 1.0 M H_2SO_4 and five times with H_2O before drying with Na_2SO_4 and solvent removal by vacuum distillation at 30 °C.

Carbon-13 NMR spectroscopy, performed on a JEOL GX-270 NMR spectrometer, was used to check the lignin samples for purity and to determine the relative proportion of carboxylic esters after methylation with diazomethane. A comparison of the quantitative ^{13}C experiments for acetylated and methylated acetylated kraft lignin indicated that for this preparation the carboxylic acid proportion was <5% of the methoxyl frequency. The "bound fraction" of $CDCl_3$ solvent, corresponding to the Wang h factor,[31] was estimated by integration of the deuterated solvent peak in a series of deuterium NMR spectra as the temperature was lowered slowly through its freezing point at −63 °C.

The kinematic viscosity of 1.00 M NaOH was measured relative to pure water using an Ubbelohde type viscometer in a constant-temperature water bath. Three temperatures around the desired temperature were used to evaluate the relative kinematic viscosity at 30 °C. This relative kinematic viscosity (1.17 times the water viscosity at this temperature) was converted to absolute using the known viscosity of water and the relative densities of water and 1.00 M NaOH at 30 °C. All other viscosities used were known values of the protonated analogues.[32,33]

Deuterated Solvents. The 1 M NaOD was prepared by weight from D_2O and NaOD (ICN Biomedicals, Cambridge, MA) under nitrogen and was not subsequently standardized. The pH of the D_2O lignin was measured at five concentrations in D_2O and H_2O. Over the concentration range used the pH (pD) of the D_2O solutions was relatively constant at $9.14 - 0.25c$ (kg m^{-3}) or $8.87 - 0.25c$ (kg m^{-3}) for an equivalent H_2O solution. The pH of the unbuffered D_2O solutions reflected the pH at which the lignin was previously freeze-dried. The pH 6.5 deuterated phosphate buffer solution was made by mixing 0.1 M KD_2PO_4 (Cambridge Isotope Laboratories, Woburn, MA) in D_2O and adjusting the pH to 6.5 using 1 M NaOD solution. All other deuterated solvents were used as obtained from Cambridge Isotope Laboratories. When unacetylated lignin was used, it was first freeze-dried in D_2O. Concentrations were measured by weight and subsequently converted to SI w/v concentrations using the appropriate deuterated solvent density and 0.655 as the lignin partial specific volume.[14] Acetylated lignins were transferred in solvent, which was removed from the NMR tube under vacuum at 30 °C. Samples were prepared in 4-mm NMR tubes.

PFGNMR Apparatus. The pulsed field gradient apparatus used is similar to the previously reported JEOL FX-60 based system.[34] However, the work reported here was carried out with a new probe incorporating a very high gradient quadrupolar coil. This coil had a calibration factor of 1.19 T m^{-1} A^{-1} and was driven by a Kepco ATE 75/15 power supply thereby providing gradients up to 10 T m^{-1}. This system enabled all measurements to be performed using spin echos formed at around 12 ms, except for

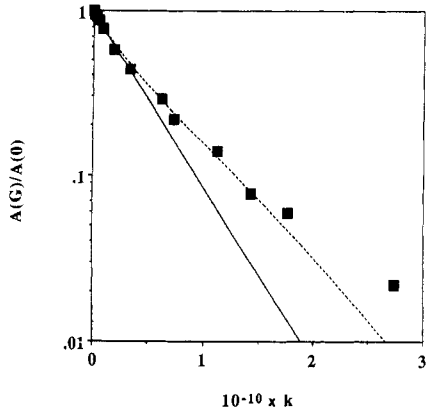

Figure 2. Typical pulsed gradient spin-echo attenuation to 1% of the zero-gradient signal for polydisperse acetylated kraft lignin M_w = 4500 in $CDCl_3$. the dashed line is the nonlinear fit to eq 4a, and the solid line is the fit to $\bar{D}_s$ in eq 4a.

some very slow diffusion measurements in which the spin echos at 32 ms were measured. All diffusion measurements were made at 30 °C. A typical echo attenuation plot for polydisperse acetylated kraft lignin in $CDCl_3$ is shown in Figure 2.

Data Analysis. The treatment of the echo attenuation using the Stejskal and Tanner equation involved several different least-squares analyses depending on the experiment and on the extent to which we desired to characterize polydispersity. Where the zero-gradient signal was collected in n acquisitions, we would typically collect and normalize $8n$ acquisitions for echos attenuated around 5–10% and $16n$ acquisitions for echos attenuated below 5%. While this method effectively reduces the errors of the most attenuated data points, the weighting of these points does not justify a linear least-squares approach to the log of the echo attenuation. As such, we used this approach only for our initial data interpretation during the pulsed field gradient experiments. In subsequent analyses a nonlinear least-squares FORTRAN program,[35] using Marquardt's gradient expansion algorithm,[36] was used to fit the data to single and double exponentials. When not otherwise specified the diffusion coefficients reported here are nonlinear fits to single exponentials, except for some of the low-concentration data from DMF, D_2O, and aqueous NaOH solutions in which double exponentials had to be used to remove the rapid solvent diffusion. In the case of the aqueous and DMF data, where the solvents had low isotopic purity, the necessity of fitting the low-concentration data to solvent and solute diffusion coefficients, differing by a factor of approximately 30, contributed to the scatter. This method of analysis and scatter may have precluded detection of small amounts of associated components with diffusion coefficients several orders of magnitude slower than the predominant solute species.

In addition to the single- and double-exponential analysis discussed above, we have also carried out an analysis that accounts for lignin polydispersity. The data from the acetylated lignin preparations were superior to those of the unacetylated lignin preparations because the weight density of protons is nearly doubled by acetylation and the deuterated solvents were of higher isotopic purity. The higher quality of the nonaqueous data permitted polydispersity analysis using moments in a modification of the approach developed for interpretation of dynamic light scattering by Koppel[37] and Pusey.[38] In this method the observed echo attenuation is viewed as a distribution of exponentials of the diffusion coefficients of the contributing lignin components:

$$A(k)/A(0) = \int_0^\infty P(D_s) \exp(-D_{sk})\, dD_s \qquad (3)$$

where $k = \gamma^2G^2\delta^2(\Delta - \delta/3)$, a function of gradient time and strength, and $P(D_s)$ is the distribution of diffusion coefficients due to polydispersity. Following Koppel, we use a MacLaurin expansion about the weight-averaged diffusion coefficient $\bar{D}_s$ in order to evaluate the moments of the distribution:

$$A(k)/A(0) = [\exp(-k\bar{D}_s)]\left[1 + \frac{\mu_2k^2}{2!} - \frac{\mu_3k^3}{3!} \ldots\right] \qquad (4a)$$

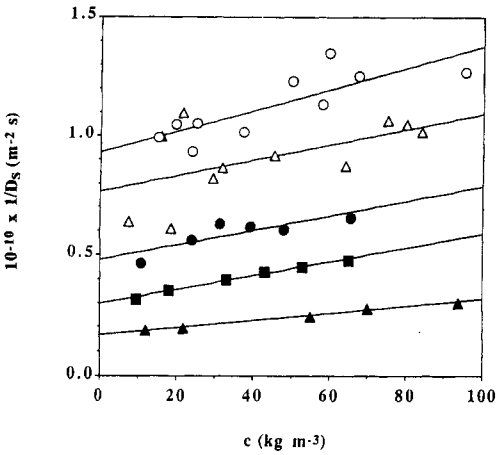

Figure 3. Concentration dependence of the self-diffusion coefficients of polydisperse kraft lignins in the dilute regime plotted versus $1/\bar{D}_s$ in order to evaluate D_0 and k_{D_s} values. Experimental points, calculated by using single-exponential nonlinear fits to eq 1, for unacetylated lignin in D_2O (○), 1 M NaOD (△), and DMF-d_7 (●) and for acetylated kraft lignin in $CDCl_3$ (■) and acetone-d_6 (▲).

from which may be derived

$$\log\{A(k)/A(0)\} = 1 - k\bar{D}_s + \frac{\mu_2k^2}{2!} - \frac{\mu_2k^3}{3!} \ldots \qquad (4b)$$

Equation 4a was used in a nonlinear fit using Marquart's gradient expansion algorithm,[36] and eq 4b was used in a signal-weighted linear least-squares fit routine LFIT found in ref 39. In order to improve the performance of the nonlinear fit of eq 4a, the experimental values for k were first multiplied by the expected $\bar{D}_s$ value. In addition, the moments were reparameterized as values relative to $\bar{D}_s$ as reported in Figure 11. In practice, the quadratic and cubic expressions give increasing statistical errors, although the systematic errors due to polydispersity are reduced by using this analysis. As shown in Figure 10, fits to eqs 4a and 4b produce similar results, although the potential for error in the analysis was greater with the linear fit to eq 4b. Figure 2 shows a nonlinear least-squares fit to eq 4a and the single-exponential $\bar{D}_s$ fit from the same equation.

The average diffusion coefficient $\bar{D}_s$ corresponds to the leading linear term of the expansion and is defined in a manner consistent with eq 2 as

$$\bar{D}_s = \int_0^\infty D_sP(D_s)\, dD_s \qquad (5)$$

In the limit as $k \to 0$, $\bar{D}_s$ becomes the initial slope of the plot of $\log\{(A(k)/A(0)\}$ vs k. Because of the expansion about $\bar{D}_s$, the first moment of the distribution is zero. The second moment then gives a measure of the width of the distribution as

$$\mu_2 = \int_0^\infty (D_s - \bar{D}_s)^2P(D_s)\, dD_s \qquad (6)$$

The third moment gives a measure of the skewness of the distribution. The scaling of the diffusion coefficients with molecular weight will enable comparison of these moments with the moments of the molecular weight distribution of the polymer.

Solvent and Concentration Dependence of Lignin Diffusion

The concentration dependence of the measured diffusion coefficients in the dilute regime is shown in Figure 3. Our initial experiments using unacetylated lignins in aqueous solvents and DMF indicated that only in the aqueous solutions at pH 6.5 did immediate (for example occurring within minutes rather than days) association occur. Using the Stokes–Einstein equation

$$D_0 = \frac{kT}{6\pi\eta_0R_h} \qquad (7)$$

along with the known solvent viscosities (see Experimental

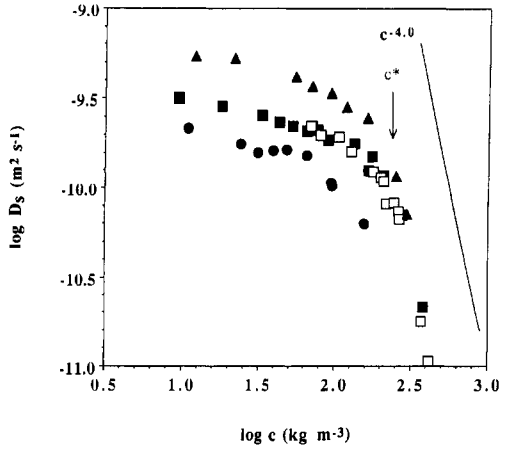

Figure 4. Concentration dependence of self-diffusion coefficients at all concentrations plotted so as to reveal scaling exponents. Polydisperse unacetylated kraft lignin in DMF-d_7 (●) acetylated kraft lignin in $CDCl_3$ (■) and acetone-d_6 (▲), and methylated, acetylated kraft lignin in $CDCl_3$ (□). Depicted in the graph are the onset of the concentrated regime at c^* and the fixed exponential concentration scaling factor of −4.

Section), we find that the average D_0 values for the kraft lignin in 1 M NaOD and D_2O correspond to an equivalent hydrodynamic radius of the lignin macromolecule of 22.8 and 20.5 Å, respectively. It should be noted that R_h is a hydrodynamic radius based on an equivalent hard sphere. The small (11%) difference in the hydrodynamic radius between pH 9 and 13 indicates that the ionization of the phenolic groups between pH 9 and 13 increases the hydrodynamic radius by swelling. This is consistent with an increase in solvent quality but otherwise it does not suggest significant association upon protonation of most of the phenolic groups. The repulsive interactions between phenolic groups therefore effectively increase the excluded volume of the lignin macromolecule. Further thermodynamic interpretation of the solvent expansion factor is dependent on the structure assumed for the polymer.[40,41]

In order to place the lignin hydrodynamic radii in context, it is instructive to compare them with those of an equivalent molar mass random coil. For random coil polystyrene in a Θ solvent we expect a 4400 M_w chain to have a radius of 15.8 Å.[42] It should be noted that care is needed in comparing the hydrodynamic size of different polymers as both the preexponential and exponential scaling factors are important. A random coil R_h will scale as $M^{0.6}$ in a good solvent, whereas a branched polymer is expected to scale with a much smaller exponent. Nevertheless, we find these lignin hydrodynamic radii broadly consistent with their measured molecular weights and find no evidence for association at these pH values. The question arises, however, as to whether there is a small but unobserved associated fraction. In this case such a component could represent a maximum of 4% based on our experience with solutions that did associate.

In view of previous reports of Rayleigh light scattering indicating that kraft lignins associated in DMF,[44] diffusion measurements were made as a function of concentration in this solvent. The data presented in Figures 3 and 4 and summarized in Table I do not indicate significant association but instead conform well to results presented here for the unacetylated lignins. Furthermore, we found that the results on the DMF solutions could be reproduced on the same sample day after day. We may note, however, that there are significant differences between the two experiments in that the light scattering experiments are usually done at higher concentrations and are also more sensitive to large molecular weight components. The signal for an associated component may have a short T_2 in the PFGNMR experiment, thus further decreasing its contribution. Nevertheless, our diffusion coefficients are over 2 orders of magnitude different from those corresponding to a radius of gyration of 740–3000 Å calculated from the light scattering data.[43,44] The PFGNMR values are a direct and accurate measure of the self-diffusion coefficient and hence reflect the radius of gyration. In the case of lignin the light scattering experiment may be complicated by absorbance and fluorescence.

In a pH 6.5 phosphate buffer the pulsed field gradient experiments exhibited greatly reduced diffusion coefficients, requiring relatively strong gradients of longer duration as shown by the echo attenuation plot shown in Figure 5. Presented in Table II are the results from these data, which were analyzed by using a nonlinear fit of one and two exponentials to characterize the average molecular weight and polydispersity. The spin-echo attenuation plots indicate a bimodal distribution as has been suggested by chromatography. This bimodal distribution is characterized by the two-exponential fits given in Table II. The diffusion coefficient D_s for these solutions of 5.48×10^{-12} m^2 s^{-1} yields a hydrodynamic radius of 380 Å. Remarkably, this corresponds to 25 000 times the volume of the 4500 moelcular weight components.

Two-exponential fits to these pH 6.5 data yielded a set of slowly diffusing components comprising 14–18% of the lignin mass with a diffusion coefficient of approximately 7.1×10^{-13} m^2 s^{-1}, which is about 1 order of magnitude slower than the D_s and approximately 200 times slower than the average diffusion coefficient at pH 9.0 and in 1 M NaOH. The hydrodynamic radii of about 380 Å for the major component and 3900 Å for the minor component correspond well to the typical and largest z-average radii of gyration found by Gupta and Goring for alkali lignins at pH 6.5 by light scattering.[16] We interpret these slow diffusion coefficients for kraft lignins in aqueous solutions at neutral pH values as corresponding to associated structures. Table II shows that the D_s values increase with increasing c. We attribute this to the precipitation of higher mass aggregated components as c increases, although it should be noted that at no stage did the measured samples become cloudy.

The D_0 values for unacetylated kraft lignin in DMF and for acetylated kraft lignin in acetone-d_6 and chloroform-d suggest a more compact molecule than that found in 1 M aqueous NaOD and also the pH 8.9 solution of D_2O as shown by the diffusion results for these solvents presented in Figures 3 and 4. More importantly, these diffusion coefficients indicate that little or no association occurs under these nonaqueous solvent conditions. Because of the lower viscosity of these solvents, the translational mobility is significantly greater than in aqueous solvents. From the values given in Table I, the analysis using single-exponential fits gives R_h values of 13.3, 13.2, and 13.1 Å for DMF, acetone, and chloroform, respectively, a surprisingly compact dimension for such a molecular weight. However, as we shall subsequently indicate, these radii should be enhanced by a factor of ca. 1.24 to correctly reflect the value applicable to lignin of mass M_w. These very small effective hydrodynamic radii suggest a significant conformational change on acetylation and solvation in the nonaqueous solvent. An independent estimate of the R_h may be obtained by calculating the radius of an equivalent compact sphere from the molar partial specific volume of lignin. This yields 10.5 Å vis the following

Table I
D_0, $\bar{R}_h$, and k_{D_s} Values

sample	solvent	M_w[a]	$10^{10}D_0$, m^2 s^{-1}	$\bar{R}_h$, Å	k_{D_s}, kg m^{-3}
kraft lignin[b]	1.0 M NaOD	4500	1.06 ± 0.04	22.9	0.005 ± 0.001
kraft lignin	D_2O	4500	1.4 ± 0.1	20.5	0.004 ± 0.002
kraft lignin	D_2O/pH 6.5	4500	0.05 ± 0.01		−0.002 ± 0.003
kraft lignin	DMF	4500	2.12 ± 0.09	13.3	0.014 ± 0.002
acetylated kraft lignin[c]	acetone-d_6	4500	5.7 ± 0.1	13.2	0.010 ± 0.004
acetylated kraft lignin[d]	acetone-d_6	4500	6.2 ± 0.2	12.1	0.0158 ± 0.0009
acetylated kraft lignin[c]	$CDCl_3$	4500	3.30 ± 0.08	13.1	0.0105 ± 0.0006
acetylated kraft lignin[d]	$CDCl_3$	4500	3.65 ± 0.04	11.8	0.0026 ± 0.0006
acetylated fraction	$CDCl_3$	7510	1.80 ± 0.07	24	0.014 ± 0.001
acetylated fraction	$CDCl_3$	4490	2.7 ± 0.1	16	0.005 ± 0.003
acetylated fraction	$CDCl_3$	2500	3.01 ± 0.08	14.3	0.009 ± 0.002
acetylated fraction	$CDCl_3$	1260	3.5 ± 0.1	12	0.003 ± 0.003
acetylated fraction	$CDCl_3$	400	4.81 ± 0.3	5	0.011 ± 0.001

[a] Molecular weight of acetylated lignins is before acetylation. [b] Viscosity values used are discussed in the Experimental Section. [c] Regression to zero concentration using D_s values from nonlinear least-squares single exponential. [d] Regression to zero concentration using $\bar{D}_s$ values from nonlinear least-squares fit to eq 4a.

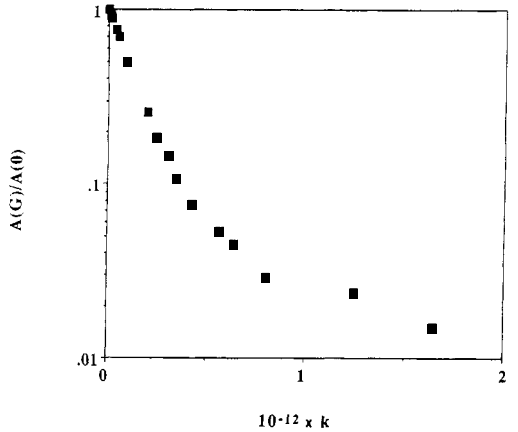

Figure 5. Typical echo attenuation plot demonstrating the high gradients and long delay times necessary for lignin solutions in pH 6.5 deuterated phosphate buffer. These data indicate large associated molecules with hydrodynamic radii of ca. 380 Å and a low polydispersity down to attenuations of ca. 8%. At this point another component an order of magnitude larger begins to dominate. Analyses for the pH 6.5 data are given in Table II.

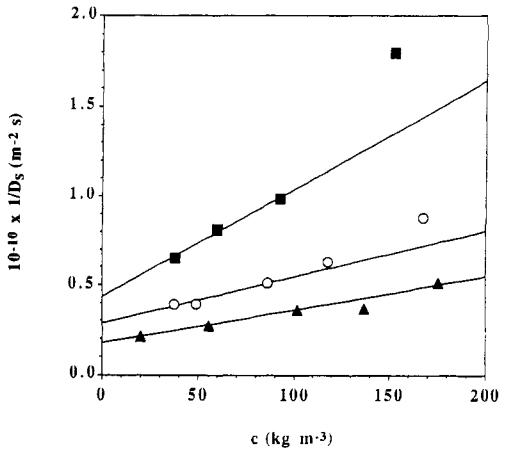

Figure 6. Representative self-diffusion coefficients in $CDCl_3$ for acetylated kraft lignin fractions of molecular weights 7510 (■), 2500 (○), and 400 (▲) plotted as a function of concentration. The lines indicated are fit, in this case, to data below 100 kg cm^{-3} to extract D_0 and k_{D_s} values; points at higher concentrations deviate from these lines as higher order interactions become important.

relation:

$$R_{h,min} = (3M\bar{V}/4\pi N_A)^{1/3} \quad (8)$$

where $\bar{V}$ is the partial specific volume and N_A is Avogadro's number.[45] Therefore, regardless of the uncertainty in the D_0 value due to polydispersity effects, we find that the experimental R_h is very near the mimumum possible radius. Given the maximum value for the R_h from Table I of 13.2 Å and the minimum possible radius of 10.5 Å, we may calculate the maximum friction factor f_s/f_{min} of 1.26. This enhancement may be due to solvation and deviations from sphericity. Perrin friction factors obtained from the D_0 values are dependent upon the axial ratio a/b, which, for an oblate ellipsoid, is[45]

$$f_s = \frac{\{(a/b)^2 - 1\}^{1/2}}{(a/b)^{2/3}\tan^{-1}\{(a/b)^2 - 1\}^{1/2}} \quad (9)$$

Given this equation and the ratio of f_s to f_{min}, we obtain a maximum asymmetry a/b of ~3. The zero-concentration limit of the friction parameter for the solute is perhaps the least sensitive method to detect solute asymmetry. Below we shall obtain a further estimate of the solute asymmetry by analysis of the concentration dependence of the solute and solvent diffusion.

Table II
Diffusion Coefficients of Kraft Lignin at pH 6.5

concn, kg m^{-3}	$10^{-12}D_s$, m^2 s^{-1}	$10^{-12}D_s$(fast),[a] m^2 s^{-1}	$10^{-12}D_s$(slow),[a] m^2 s^{-1}	amplitude D_s(fast), %
17	5.0	6.2	0.61	91
48	5.4	7.3	0.93	86
62	4.8	5.7	0.43	92
78	6.6	7.7	0.85	87

[a] Two-exponential nonlinear fit.

Scaling of D_0 with Molecular Weight

The success of the fractionation procedure using Superose and 0.1 M NaOH enabled the D_0 diffusion coefficient of the lignin macromolecules to be measured as a function of molecular weight. The scaling here relies on the accuracy of the previously reported sedimentation equilibrium calibration of a Superose size exclusion column.[8] Representative diffusion coefficients of these fractions as a function of concentration in chloroform are presented in Figure 6. The diffusion coefficients of fractions in 1 M NaOH showed less concentration dependence and were more difficult to reproduce and are therefore reported in Figure 7 with the extrapolated D_0 chloroform values as average values of three measurements under 5% w/v. The results give scaling relations of $D \sim M^{-\alpha}$ in the two solvents as the slope of the given lines in the log–log plot. The molecular weight scaling exponents

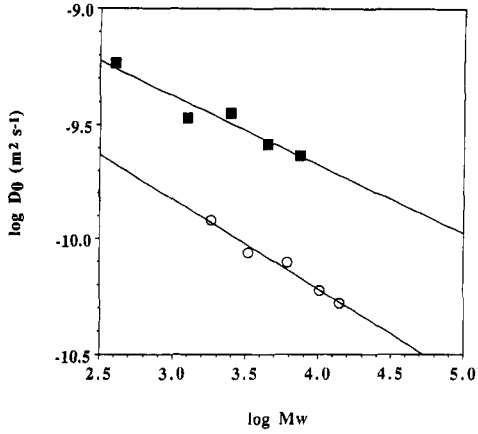

Figure 7. Scaling of diffusion coefficients with molecular weight for unacetylated lignin fractions in 1 M NaOH (○) and acetylated lignin fractions in $CDCl_3$ (■). The lines fit to the data give molar mass scaling exponents of 0.30 in $CDCl_3$ and 0.39 in 1 M NaOD, indicative of a highly branched macromolecule.

of 0.39 in 1 M NaOH and 0.30 in $CDCl_3$ are much smaller than the values of 0.5 for a random coil in a Θ solvent and 0.6 for a random coil in a good solvent.[41] The expected exponent for a particle of uniform internal density is 0.33.[45] This is very close to the value obtained for acetylated lignin in chloroform. The larger exponent of 0.39 for 1 M NaOH is consistent with the initial conclusion for the D_0 values that the lignin assumes an expanded conformation in aqueous solvent.

These small molecular weight exponents along with the very compact size are indicative of a branched macromolecule or a remarkably compact secondary and tertiary structure. Remarkably, Gupta and Goring's viscosity and sedimentation data on alkali lignins with molecular weights between 5×10^4 and 5×10^7 (measured at pH 9.65) also indicated a molecular weight dependence between that expected for a compact sphere and a random coil.[16] This correspondence between separate data at different molecular weights indicates a uniform density of phenylpropane groups in both high and low molecular weight structures. In principle, one may obtain a measure of the degree of branching of the lignin macromolecule by comparing the radii with the equivalent values for a linear chain as has been done for the radii of gyration[47,48] or for diffusion coefficients.[49] Unfortunately, we have no way of knowing the effective radius of an equivalent linear molecule. Recent results indicate that star polymers with up to 18 branches scale to the same molecular weight exponent as linear polymers,[48] the differences in the radius of gyration corresponding only to preexponential factors. Diffusion measurements on star polymers have also shown that the differences in the diffusion coefficients that determine the Stockmayer–Fixman h parameter, a ratio of diffusion coefficients of linear and branched polymrs, also correspond to the preexponential scaling factor rather than the molecular weight scaling exponent.[49] These results indicate that star polymers do not approximate the lignin macromolecule well. One possible explanation for the differences in exponents in the aqueous and nonaqueous solvents is that in aqueous solvents, segments of the polymer are free to adopt a random coil conformation around the outside of the branched core. This would have the effect of both dramatically increasing the hydrodynamic radius as observed and raising the mean exponent observed in D_0 vs M scaling.

Solvent Diffusion

In order to better understand the asymmetry of the kraft lignin macromolecule in solution, we measured the diffusion coefficient of the solvent as a function of lignin concentration, using protonated solvents. The analysis of solvent diffusion to obtain macromolecular shape factors is based on the differing obstruction presented by solute molecules of differing shape.[31] There are two principal difficulties with the model. First, it is based on a depiction of the macromolecule as an impenetrable object. This is only accurate in the non-free-draining limit. Second, it accounts for the effect of solvent molecule binding by the introduction of a solvation parameter. This parameter is notoriously difficult to determine independently.[41] Despite the difficulties in defining and measuring the solvation parameter, the shape factor is particularly valuable for oblate ellipsoids where the platelike macromolecules can provide substantial barriers to a solvent molecule and also the influence of the solvation term is less significant. By contrast, a prolate ellipsoid provides an obstruction that tends to one-dimensional and so has a less pronounced effect on the diffusion coefficient of macromolecules. In this case the uncertain solvation term can prove to be a dominate influence.

The attenuation of the zero-concentration diffusion coefficients of solvent molecules may be written as

$$D = D_0 \frac{(1 - \bar{\alpha}\phi)(1 - f)}{1 - \phi} \tag{10a}$$

where the volume fraction of "hydrated" macromolecules is a function of the partial specific volume of the macromolecule $\bar{V}$, the hydration parameter h, the solvent density d_0, and the weight fraction of the macromolecule w:

$$\phi = \frac{\bar{V} + h/d_0}{\bar{V} + \{(1 - w)/wd_0\}} \tag{10b}$$

The fraction of solvent that is immobilized is $f = h[w/(1 - w)]$. Using the binomial approximation with rearrangement, we may rewrite this equation as[52]

$$D = D_0\{1 - w[(\bar{\alpha} - 1)(\bar{V}_{d0} + h) + h]\} \tag{11}$$

The shape factor, $\bar{\alpha}$, is a function of the axial ratio a/b and for an oblate ellipsoid is very sensitive to this ratio. Consequently, $\bar{\alpha} - 1$ may dominate h. We estimated the solvation of the acetylated lignin in chloroform by measuring the total NMR signal of the solvent as the temperature was lowered through the freezing point to −80 °C. These measurements suggest $h \approx 0$ as effectively all of the deuterium signal was frozen out below the freezing point. It is uncertain that the unfrozen fraction of solvent accurately reflects the h factor. In the Wang model h depends upon a solvation sphere of several layers of molecules that become less correlated with the inner layers at increasing distances. Our h value is in contrast to solvent freezing and hydrodynamic experiments on polysaccharides and globular proteins that give finite h values between 0.2 and 1.[37,42] From the slope of 3.97 in Figure 8 and an h factor of 0, we obtain a value of $\bar{\alpha}$ of 4.9, which requires the shape to be oblate rather than prolate and with an axial ratio a/b of about 18.

Concentration Dependence in the Dilute Regime

Pulsed gradient spin-echo NMR measures the molecular self-diffusion coefficient, for which concentration effects enter through the friction term. In this regard it should be noted that the polymer friction coefficient which applies

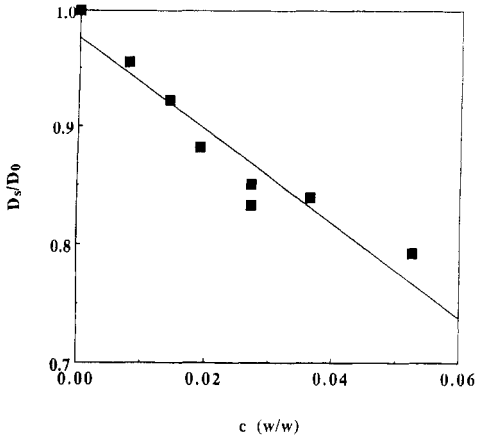

Figure 8. Plot of the relative diffusion coefficient of the solvent $CHCl_3$ as a function of concentration used to calculate the eccentricity of the lignin macromolecule. Following the theory of Wang,[31] this severe attenuation of the solvent diffusion with increasing concentration indicates a highly eccentric oblate ellipsoid.

in sedimentation and mutual diffusion must be distinguished from that applicable to self-diffusion.[53] This has been demonstrated experimentally in comparative measurements on random coil polymers in good solvents.[54] The standard formalism used to incorporate concentration effects in the dilute regime is given by

$$D_s = k_B T/f \tag{12}$$

where f is the friction coefficient. Pulsed field gradient NMR measures the self-diffusion coefficient in which there are no thermodynamic effects; therefore the second virial term is dropped, and the only concentration effects are contained within the friction term as[55]

$$f = f_0(1 + k_{D_s}c + ...) \tag{13}$$

The macromolecular friction coefficient at infinite dilution, f_0, is given by the familiar Stokes relation expressed in terms of the hydrodynamic radius as $f_0 = 6\pi\eta_0 R_H$. Consequently, a plot of $(D_s/D_0)^{-1}$ versus concentration can be used to derive the first-order concentration dependence coefficient, k_{D_s}. k_{D_s} can then be used to obtain information concerning hydrodynamic interactions between molecules. These interactions depend on solute conformation.

There are two principal approaches in the theory of k_{D_s}. The case of random coils the concentration effect mostly arises from the dependence of the radius of gyration on the separation of polymer pairs. This model is not appropriate to the case of lignin, which is both branched and compact. The second approach concerns the interparticle hydrodynamic and direct potential perturbations to motion, and in the non-free-draining limit of the hard sphere, the Brownian motion has been analyzed by a number of authors.[53,56] Since the hydrodynamic effect varies as R^{-1}, where R is the interparticle separation, this influence will dominate in the dilute regime compared with the hard-sphere potentials, which have a significantly sharper distance dependence. This hydrodynamic effect has been treated in detail by Anderson and Reed,[57] who calculate the velocity U_1 of a particle according to the one-dimensional Langevin equation:

$$M\frac{dU_1}{dt} = -fU_1 + B(t) \tag{14}$$

where M is the particle mass, f is the friction factor, and $B(t)$ is the fluctuating force. The velocity is then calculated by integrating over the volume v:

$$\langle U_1 \rangle = U_{10} - c\int_v g(r)(U_{10} - U_{12})\,dv \tag{15}$$

where c is a function of the concentration and $g(r)$ is the equilibrium radial distribution function. The velocity of the particle is U_{10} without any interactions and U_{12} in the presence of sphere 2. Callaghan and Lelievre's modification of this model allows for the effect of shape on the interaction between particles.[58] Their model assumes orientational averaging during interaction between particles and is applicable for large axial ratios only. This model does not modify the forces constituting the interaction between two particles but merely averages the distances to which they apply over different shaped molecules. Callaghan and Lelievre's model results in an enhancement of the k_{D_s} by a factor of $0.35(a/b)$ for prolate ellipsoids and $0.19(a/b)$ for prolate ellipsoids.

Theoretical values for k_{D_s} are generally expressed in terms of the volume fraction ϕ. In the Anderson and Reed model the k_{D_s} is of order 2, while the Akcasu model for random coils predicts $k_{D_s} \approx 1$. Conversion to w/v concentration based units, c, requires a knowledge of the molecular hydrodynamic volume, ν_m via

$$k_{D_s}{}^c = k_{D_s}{}^\phi \nu_m N_A M^{-1} \tag{16}$$

Because the hydrodynamic radius of the random coil incorporates a significant solvent component, $k_{D_s}{}^c$ is expected to be considerably larger than the $k_{D_s}{}^c$ for the equivalent molar mass branched polymer with a spherical conformation. For example, the spherical, branched carbohydrate glycogen has $k_{D_s}{}^c \sim 0.001$ kg^{-1} m^3 in D_2O and DMSO, whereas the random coil carbohydrate dextran has $k_{D_s}{}^c \sim 0.03$ kg^{-1} m^3 in these solvents.[58] The low value for glycogen suggests that the hydrodynamic volume ν_m is consistent with a highly compact structure in which ν_m is best represented by using the partial specific volume $\bar{V}$. Our own estimates of the hydrodynamic volume of lignin based on D_0 measurements suggest a similarly compact molecule. By contrast, however, the $k_{D_s}{}^c$ value given in Table I for acetylated kraft lignin in acetone-d_6 and $CDCl_3$ is much higher than that expected for a sphere. Using the oblate ellipsoid hydrodynamic model above, we find a/b for acetylated lignin of around 20. Similar deviation from the spherical $k_{D_s}{}^c$ value for branched macromolecules has been seen in the case of the carbohydrate amylopectin.[58] This molecule has $k_{D_s}{}^c$ values of 0.03 and 0.27 respectively in D_2O and DMSO, illustrating the influence of shape in the hydrodynamic interaction.[58]

Semidilute/Concentrated Regimes

At higher concentrations the volume available for each polymer molecule is restricted by the presence of other polymer molecules. Above this concentration, term c^*, the diffusion coefficient dramatically decreases. An estimate of c^* enables the radius of the largest molecular diameter a to be calculated via

$$c^* = MN_A{}^{-1}(2a)^{-3} \tag{17}$$

We have indicated c^* for polydisperse acetylated lignin in chloroform-d and acetone-d_6 on Figure 4 at ca. 200 mg m^{-1}. This value gives an effective radius of 16.7 Å, which is in fair agreement with the hydrodynamic radius calculated from the D_0 value of 13.2 Å. The smaller value of the hydrodynamic radius is consistent with a nonspherical conformation.

In the concentrated regime, the diffusion coefficients scale approximately as c^{-4} as shown in Figure 4. This is

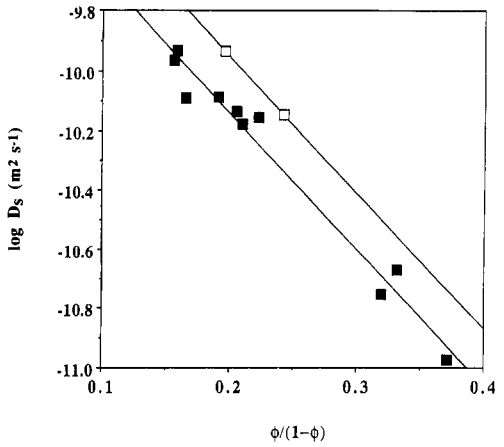

Figure 9. Plot of diffusion coefficients above c^* versus the ratio of macromolecular volume to free volume as given by eq 18. Acetylated lignin fractions in $CDCl_3$ (■) and acetone-d_6 (□).

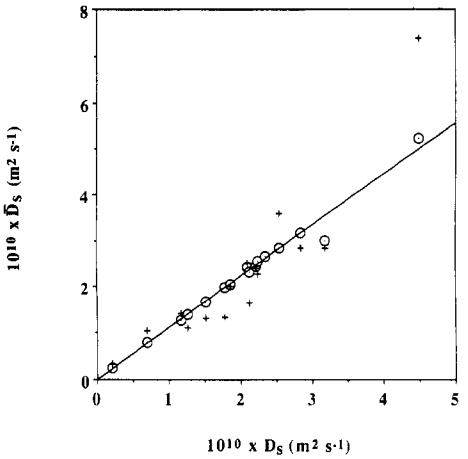

Figure 10. Single-exponential nonlinear least-squares fit to D_s versus the average diffusion coefficient $\bar{D}_s$ as calculated by eq 4a (○) and 4b (+) for acetylated lignin fractions in $CDCl_3$. The line is fitted to the data analyzed by using eq 4a. This fit illustrates the higher correlation of the single-exponential analyses with the fit to eq 4a as compared to the fit using eq 4b. $\bar{D}_s$ values are 1.12 times faster than the single-exponential D_s values.

considerably steeper than in the case of random coil polymers, where concentration scaling ranges from −1.75 for a good solvent to −3 for a Θ solvent.[59,60] In the present case of compact and apparently branched molecules with a weight-average degree of polymerization of ca. 24, we see little opportunity for entanglement as a theoretical basis for this scaling. Remarkably similar scaling behavior has been previously reported for amylopectin in DMSO.[42] This polymer also exhibited a concentration exponent of ca. −4. Furthermore, an identical c^* value of 200 kg m^{-3} was apparent despite the fact that the molecular weight of the amylopectin was on the order of 10^6. The c^* concentration gives a relative density of macromolecule based on weight concentration. Apparently, both amylopectin and the acetylated kraft lignin occupy roughly the same volume per unit weight when in solution.

Self-Diffusion of Branched Macromolecules above c^*. Given that the concentration scaling for two different branched macromolecules agrees, it is interesting to speculate on the likely mechanism for self-diffusion by application of free-volume theory.[61-65] Within this theory, the dense and close-packed macromolecules present obstacles to self-diffusion rather similar to those of small molecules in the pure liquid. In the latter case the surrounding molecules form a cage that allows substantial translational motions only when the free volume has recognized to allow a space for movement on the order of one molecular dimension. Originally, this theory was developed by Cohen and Turnbull to describe diffusion in simple liquids.[61] Subsequently, it was developed by Fujita[64] and others for application to polymer solutions. Recent reviews of the theoretical and experimental aspects of the application of free-volume theory to the thermodynamics[65] and diffusion of polymer solutions have been published.[62,63] As a first approximation, we have used a simplified version of this approach for the concentrated macromolecules in solution where the free volume is taken to be the space occupied by the solvent molecules.

In the Cohen and Turnbull depiction of Brownian motion based on free-volume effects, the self-diffusion coefficient is given by[61]

$$D_s = a \exp\{-\gamma v^*/v_f\} \qquad (18)$$

where v_f is the free volume, v^* is the molecular volume, and γ is a geometric factor. In our application of this approach to macromolecules, we assign the molecule to free volume ratio as $\phi/(1-\phi)$. A nine-parameter version of this equation has been presented by Ventras and Duda[62,63] but their approach is more appropriately suited to synthetic polymers with more precisely known structural and thermodynamic properties. It is clear that eq 18 does not represent a scaling with a concentration to a fixed exponent. Nonetheless, the relationship does provide a steep concentration dependence as required, and over a small concentration range, as in the present case, it can yield an apparent exponent close to 4 provided the geometrical factor γ is suitably chosen. Figure 9 shows the theoretical line arising from eq 18, which yields a value of γ of 4.58. The agreement with the data is good. It is likely that the apparent γ value obtained by such an approach may yield information on macromolecular shape factors. We have not attempted such an analysis here but we note the similarity between apparent γ's for lignin and amylopectin. It is likely therefore that lignin exhibits a similar shape factor to amylopectin, a macromolecule that is known to be highly oblate.

Polydispersity: Moment Analysis

Moment analysis provides a method of dealing with the polydispersity of the lignin sample without assuming any particular molecular weight distribution. Both linear (eq 4b) nonlinear (eq 4a) quadratic and cubic cumulant analyses give diffusion coefficients about 1.12 times faster than the single-exponential analysis regardless of the concentration. However, the application of linear eq 4b resulted in considerably more scatter in $\bar{D}_s$ values when compared to concentration or D_s as shown in Figure 10. The constant ratio indicates that the concentration scaling is independent of the choice of methods for data analysis.

The trade-off between systematic error and statistical error in the application of cumulant analyses is well-known.[37,38] Statistical errors become particularly evident in the analyses of pulsed gradient spin-echo NMR where nonlinear fits on relatively few points are particularly unstable. Figure 11 shows a representative plot of the second and third moments calculated from the cubic analysis. We find the cubic analyses predict slightly lower polydispersity, although they are thought to be more accurate in predicting second-moment values.[37] These analyses show an average second moment for the polydisperse lignin in $CDCl_3$ of approximately 0.3, and despite considerable scatter these values generally increase with decreasing diffusion coefficients. As shown in Figure 11,

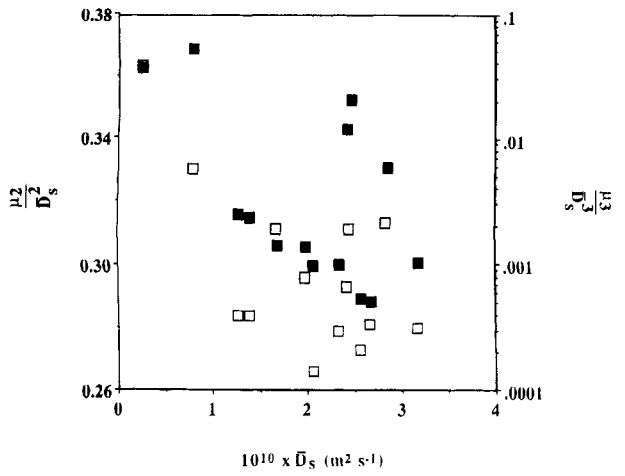

Figure 11. Average diffusion coefficient $\bar{D}_s$ compared to second (□) and third (■) moments of the self-diffusion coefficients as calculated by the cubic moment analysis (eq 4a) for acetylated lignin fractions in $CDCl_3$. The points indicate a trend toward higher apparent polydispersity under more concentrated conditions.

the third moment has a much steeper dependence on the concentration which may be approximated as exponential. This variation in the apparent polydispersity could be due to the variation of the diffusion coefficient molecular weight scaling at higher concentrations, accentuating the variation between different components.

If we assume a log-normal distribution and a scaling relationship between self-diffusion and molar mass, we may then calculate the contribution of polydispersity index to D_s and to the second moment of the diffusion analyses with the experimental size exclusion value. The molecular weight distribution $P(L)$ becomes a function of the peak value of the molar mass and σ, the standard deviation of the distribution width:

$$P(L) = (\pi\sigma^2)^{-1/2} \exp\left[-\left\{\frac{L - L^0}{\sigma}\right\}^2\right] \tag{19}$$

where $L = \ln(M)$. This distribution simplifies the calculation of the number- and weight-average molecular weights to[66]

$$M_n = M_0 \exp(\sigma^2/4) \tag{20}$$

$$M_w = M_0 \exp(3\sigma^2/4) \tag{21}$$

The polydispersity ratio then becomes

$$M_w/M_n = \exp(\sigma^2/2) \tag{22}$$

It can be shown that, for the scaling relation $D_s(M) = aM^{-\alpha}$, the average diffusion coefficient calculated with the moment expansion is[66]

$$\bar{D}_s = D_s(M_w) \exp\left\{\frac{[\alpha(\alpha+2) - 3\alpha]\sigma^2}{4}\right\}$$

$$= D_s(M_w)(M_w/M_n)^{\alpha(\alpha-1)/2} \tag{23}$$

For example, in the lignin dilute regime where $\alpha \simeq 0.3$ and assuming $M_w/M_n \simeq 3$, eq 23 predicts

$$\bar{D}_s = 1.24 D_s(M_w)$$

The second moment may be written as

$$\mu_2 = \bar{D}_s^2[(M_2/M_n)^{\alpha^2} - 1]$$

With the dilute-regime exponent of −0.3, the average second moment (reported as $\mu_2\bar{D}_s^2$) of 0.4 yields $M_w/M_n \simeq 1.8$. This is lower than the value of ~3 obtained from GPC. This discrepancy may reflect the presumption of a log-normal distribution.

Conclusions

The hydrodynamic radii of acetylated and unacetylated polydisperse kraft lignins calculated from diffusion coefficients in nonaqueous and aqueous solvents show excellent agreement. The exceptions to this agreement were measurements in dilute solution at pH 6.5, where the diffusion coefficients are 25 times slower than the corresponding value in alkaline solution. The relatively rapid diffusion coefficients measured at pH 9 suggest that some of the necessity of using very high pH solutions for chromatography of kraft lignin components may be due to lignin–column interactions rather than lignin–lignin association. The difference in the diffusion coefficients of kraft lignin in alkaline and near-neutral pH conditions corresponds to an increase in the average volume of over 4 orders of magnitude. Our data indicate that the protonation necessary to permit rapid association predominantly occurs between pH 9.0 and 6.5. This is in agreement with ultracentrifuge studies using dilute solutions of kraft lignins at pH 9.5[10] but in contrast to light scattering data indicating that extensive association occurred immediately below pH 11.5, which is taken to be the average pK_a of kraft lignin by Woerner.[67] Unfortunately, we do not know the extent to which the pK_a of kraft lignin may be perturbed by the association process during which phenolic protons may become hydrogen bonded and buried within the relatively immense associated structure. This possible stabilization of the pK_a by association could lead to lignin dissociation as the pH is increased above 11.5 but not associating until the pH is decreased below pH 9.0. In Woerner's case the pH was increased and in our case the pH was decreased. Further diffusion measurements at pH values between 7 and 12 could clarify the interdependence of phenolic protonation and association. Additionally, we may note, concerning conflicting experimental results for the hydrodynamic radius in DMF,[43,44] that the extent to which the lignin is protonated before freeze-drying may play a decisive role in its subsequent associative behavior in DMF.

Size exclusion chromatography experiments have previously shown that random coil poly(styrenesulfonates) have larger hydrodynamic radii than kraft lignins and therefore elute at smaller retention volumes than the corresponding lignin fractions of the same molecular weight.[68] Given the great differences in the scaling of hydrodynamic radius between random coil and branched polymers, efforts to make cross comparisons of volume–molecular weight relationships between other polymers and lignin are subject to substantial errors. Nevertheless, poly(styrenesulfonates) continue to be used to "calibrate" size exclusion columns for the study of lignin properties.[68] Substitution of random coil polymers for lignin in volume-dependent analyses will nearly always result in underestimation of the molecular weight of the lignin. It has been previously indicated that for kraft lignins, the linear log M_w vs retention volume size exclusion behavior was incompatible with a molecular weight independent branching index.[10] Although we are not able to speculate on the regularity of the branching, our data consistently indicate a very compact branched macromolecule.

We have obtained the molecular weight dependency of the hydrodynamic radius in 1.0 M NaOH and $CDCl_3$, both of which are consistent with a very compact branched macromolecule. The values obtained, 0.39 and 0.30, are

much smaller than similar exponential values for random coil macromolecules. Indeed, the dimensions of the acetylated lignin in $CDCl_3$ are close to the minimum possible given the molecular mass and the partial specific volume. We find that for freshly prepared lignin solutions there are few if any carboxylic groups and the hydrodynamic properties are not affected by methylation. The compact and branched macromolecular structure suggests that the short T_2 NMR relaxation times for all lignin preparations are due to long correlation times arising from low internal mobility resulting primarily from the branched structure and not from association as previously proposed.[7]

Our Wang analysis of the diffusion data of $CHCl_3$ in a solution of polydisperse acetylated lignin yields the concentration dependence of the diffusion coefficient which predicts that the lignin macromolecule is an oblate ellipsoid with an axial ratio of 18. This is in agreement with our analysis of k_{D_s} following the theory of Anderson and Reed as modified by Callaghan and Lelievre which gives an axial ratio of 20. Although all experimental evidence indicates an eccentric macromolecular shape, we must view these numbers as maximum values, as indeed the D_0 values do predict such large axial ratios using the Perrin equations.

Although the Perrin equations provide a method of analysis of ellipsoidal macromolecular shape in the zero-concentration limit, there is a sparse theoretical background for evaluation of the effects of hydrodynamic interactions between non-free-draining ellipsoids of revolution in the dilute regime on translational or rotational diffusion coefficients. Despite these deficiencies, we have found reasonable agreement between Wang analysis of solvent diffusion and an elementary theory for the interpretation of k_{D_s}. Additionally, we find that the scaling laws for random coil macromolecules are not appropriate to branched macromolecules because of the virtual impossibility of entanglement of these molecules and also because the concentration dependence scales with a higher exponent than typically found for random coils. We have proposed an interpretation of the translational mobility of hard macromolecular ellipsoids of revolution in concentrated solutions which is analogous to that given for simple liquids by Cohen and Turnbull.

Acknowledgment. T.M.G. is indebted to the National Science Foundation for support through the U.S.–Industrialized Countries Program for the Exchange of Scientists and Engineers (Grant No. INT-8701844) and to Massay University for additional financial assistance. Funding for apparatus and expendables was provided by PAPRO (Pulp and Paper Research Organization of New Zealand). Peter Daivis is acknowledged for his advice on the polydispersity analyses.

References and Notes

(1) Lewis, N. G.; Yamamoto, E.; Wooten, J. B.; Just, G.; Ohashi, H.; Towers, G. H. N. *Science* **1987**, *237*, 1344.
(2) Atalla, R. H.; Agarwal, U. P. *Science* **1985**, *227*, 637.
(3) Garver, T. M., Jr.; Sarkanen, S. In *Renewable-Resource Materials*; Carraher, C. F., Jr., Sperling, L. H., Eds.; Plenum: New York, 1986.
(4) Forss, K.; Fremer, K.-E. *Appl. Polym. Symp.* **1983**, *37*, 531.
(5) Adler, E. *Wood Sci. Technol.* **1977**, *11*, 169.
(6) Gierer, J. *Holzforschung* **1982**, *36*, 43, 55.
(7) Garver, T. M., Jr.; Sarkanen, S. *Holzforschung* **1986**, *40* (*Suppl.*), 93.
(8) Garver, T. M., Jr.; Lewis, J.; Conway, J., submitted to Holzforschung.
(9) Goring, D. A. I. Polymer Properties of Lignin and Lignin Derivatives. In *Lignins: Occurrence, Formation, Structure and Reactions*; Sarkanen, K. V., Ludwig, C. H., Eds.; Wiley-Interscience: New York, 1971.
(10) Sarkanen, S.; Teller, D. C.; Abramowski, E.; McCarthy, J. L. *Macromolecules* **1982**, *15*, 1098.
(11) Sarkanen, S.; Teller, D. C.; Stevens, D. C.; McCarthy, J. L. *Macromolecules* **1984**, *17*, 2588.
(12) Garver, T. M., Jr., to be submitted.
(13) Benko, J. *Tappi* **1964**, *47*, 508.
(14) Gupta, P. R.; Goring, D. A. I. *Can. J. Chem.* **1960**, *38*, 248.
(15) Gupta, P. R.; Robertson, R. F.; Goring, D. A. I. *Can. J. Chem.* **1960**, *38*, 259.
(16) Gupta, P. R.; Goring, D. A. I. *Can. J. Chem.* **1960**, *38*, 270.
(17) Goring, D. A. I. *Cellulose Chemistry and Technology*; ACS Symposium Series, 48; American Chemical Society: Washington, DC, 1977; p 273.
(18) Favis, B. D.; Goring, D. A. I. *J. Pulp Pap. Sci.* **1984**, *10*, J139.
(19) Yean, W. Q.; Rexanowich, A.; Goring, D. A. I. In *Chim. Biochim. Lignine, Cellul. Hemicellul., Actes Symp. Int., 1964 (1965)*, p 327.
(20) Hahn, E. L. *Phys. Rev.* **1950**, *80*, 580.
(21) Carr, H. Y.: Purcell, E. M. *Phys. Rev.* **1954**, *94*, 630.
(22) Stejskal, E. O.; Tanner, J. E. *J. Chem. Phys.* **1965**, *42*, 288.
(23) Callaghan, P. T. *Aust. J. Phys.* **1984**, *37*, 359.
(24) von Meerwall, E. D. *Adv. Polym. Sci.* **1983**, *54*, 1–30.
(25) von Meerwall, E. D. *Rubber Chem. Technol.* **1985**, *58*, 527.
(26) Stilbs, P. *Prog. NMR Spectrosc.* **1987**, *19*, 1.
(27) Kärger, J.; Pfeifer, H.; Heink, W. *Adv. Magn. Reson.* **1988**, *12*, 1.
(28) Callaghan, P. T.; Pinder, D. N. *Macromolecules* **1983**, *16*, 968.
(29) deBoer, T. J.; Backer, H. J. *Organic Synthesis*: Rabjohn, N., Ed.; Wiley: New York, 1963; Collect. Vol. 4, p 250–253.
(30) Garver, T. M., Jr. Ph.D. Thesis, University of Minnesota, 1988.
(31) Wang, J. H. *J. Am. Chem. Soc.* **1954**, *76*, 4755.
(32) Weast, R. C., Ed. *CRC Handbook of Chemistry and Physics*, 69th ed.; Chemical Rubber Publishing Co.: Boca Raton, FL, 1988; p F-41.
(33) Dreisbach, R. R. *Physical Properties of Chemical Compounds*; Advances in Chemistry 29; Amercian Chemical Society: Washington, DC, 1961; Vol. III, p 444.
(34) Callaghan, P. T.; Trotter, C. M.; Jolley, K. W. *J. Magn. Reson.* **1980**, *37*, 247.
(35) Bevington, Philip, R. *Data Reduction and Error Analysis for the Physical Sciences*; McGraw-Hill: New York, 1969; pp 235–245.
(36) Marquardt, D. W. *J. Soc. Ind. Appl. Math.* **1963**, *11* (2), 431.
(37) Koppel, D. E. *J. Chem. Phys.* **1972**, *57*, 4814.
(38) Pusey, P. N. Macromolecular Diffusion. In *Photon Correlation and Light Beating Spectroscopy*; Cummins, H. Z., Pike, E. R., Eds.; Plenum: New York, London, 1973; pp 387–428.
(39) Press, W. H.; Flannery, B. P.; Teukolsky, S. A.; Vetterling, W. T. *Numerical Recipes. The Art of Scientific Computing*; Cambridge University Press: Cambridge, 1986.
(40) Flory, P. J. *Principles of Polymer Chemistry*; Cornell University Press: Ithaca, NY, 1953.
(41) Doi, M.; Edwards, S. F. *The Theory of Polymer Dynamics*; Clarendon Press: Oxford, 1986; Chapter 4.
(42) Maa, Y. F.; Chen, S. H. *Macromolecules* **1988**, *21*, 1176.
(43) Dutta, S.; Garver, T. M., Jr.; Sarkanen, S. In *Lignin: Properties and Materials*, ACS Symposium Series: Glasser, W.; Sarkanen, S., Eds.; American Chemical Society: Washington, DC, 1988.
(44) Dutta, S. Masters Thesis, University of Minnesota, Minneapolis, 1988.
(45) Tanford, C. *Physical Chemistry of Macromolecules*; Wiley: New York, London, Sydney, 1961; Chapter 5.
(46) Bywater, S. Preparation and Properties of Star-Branched Polymers. *Adv. Polym. Sci.* **1979**, 30.
(47) Freed, K. F. *Renormalization Group Theory of Macromolecules*; Wiley: New York, 1987; pp 221–223.
(48) Bauer, B. J.; Fetters, L. J.; Graessley, W. W.; Hadjichristidis, N.; Quack, G. F. *Macromolecules* **1989**, *22*, 2337.
(49) Xuenin, C.; Zhongde, X.; von Meerwall, E.; Seung, N.; Hadjichristidis, N.; Fetters, L. J. *Macromolecules* **1984**, *17*, 1343.
(50) Stockmayer, W. H.; Fixman, M. *Ann. N.Y. Acad. Sci.* **1953**, *57*, 334.
(51) Clark, M. E.; Burnell, E. E.; Chapman, N. R.; Hinke, J. A. M. *Biophys. J.* **1982**, *39*, 289.
(52) Callaghan, P. T.; Lelievre, J. *Biopolymers* **1985**, *24*, 441.
(53) Akcasu, A. Z. *Polymer* **1981**, *22*, 1169.
(54) Callaghan, P. T.; Pinder, D. N. *Polym. Bull.* **1981**, *5*, 305.
(55) Yamakawa, H. *J. Chem. Phys.* **1962**, *36*, 2995.
(56) Berne, B. J.; Pecora, R. *Dynamic Light Scattering*; Wiley-Interscience: New York, London, Sydney, Toronto, 1976; Section 13.5.
(57) Anderson, J. C.; Reed, C. C. *J. Chem. Phys.* **1976**, *64*, 3240.
(58) Callaghan, P. T.; Lelievre, J. *Anal. Chim. Acta* **1986**, *189*, 145.
(59) Callaghan, P. T.; Pinder, D. N. *Macromolecules* **1984**, *17*, 431.
(60) de Gennes, P.-G. *Macromolecules* **1976**, *9*, 594.

(61) Cohen, M. H.; Turnbull, D. *J. Chem. Phys.* **1959**, *31*, 1164.
(62) Vrentas, J. S.; Duda, J. L.; Ling, H.-C. *J. Polym. Sci., Polym. Phys. Ed.* **1985**, *23*, 275.
(63) Vrentas, J. S.; Duda, J. L.; Ling, H.-C.; Hou, A.-C. *J. Polym. Sci., Polym. Phys. Ed.* **1985**, *23*, 289.
(64) Fujita, H. *Fortschr. Hochpolym. Forsch.* **1961**, *3*, 1.
(65) Doolittle, A. K. *J. Appl. Polym. Sci.* **1980**, *25*, 2305.
(66) Callaghan, P. T.; Pinder, D. N. *Macromolecules* **1985**, *18*, 373.
(67) Woerner, D. L.; McCarthy, J. L. *Macromolecules* **1988**, *21*, 2160.
(68) Himmel, M. E.; Oh, K. K.; Quigley, D. R.; Grohmann, K. *J. Chromatogr.* **1989**, *467*, 315.

Registry No. Kraft lignins, 8068-05-1.